

# AUTOMATIC CAR STEERING USING ROBUST UNILATERAL DECOUPLING

Jürgen Ackermann<sup>1</sup> Wolfgang Walter  
Tilman Bünte

*German Aerospace Center  
Institute of Robotics and Mechatronics  
D-82234 Oberpfaffenhofen  
Germany*

**Abstract:** In this paper a steering controller is derived using robust unilateral decoupling control. By this method automatic car steering can be split into two subtasks: a) good lane tracking of a point mass for stepwise change of the curvature of the lane reference and for lateral force disturbances and b) good yaw stabilization in the presence of yaw torque disturbances. In the design process the track following controller and the controller stabilizing the yaw rate are designed separately. A Daimler Benz City Bus O 305 used in the Prometheus program and a Pontiac 6000 STE Sedan used in the PATH program give the practical background. In the latter case with higher velocities gain scheduling by the velocity is used. Simulations for these two cars illustrate the advantages of the developed structure.

**Keywords:** Automatic Steering, Automotive/Robust Control, Robust Decoupling

## 1. INTRODUCTION

Various controller structures and design approaches have successfully been applied to automatic car steering (see e.g. Ackermann and Sienel, 1990, or Guldner, *et al.*, 1999). These two projects are used to evaluate the idea of robust unilateral decoupling (Ackermann, *et al.*, 2002). By this approach it is possible to split automatic car steering into two independent subtasks: lane tracking and stabilization of the yaw rate which are discussed in sections 3 and 4, respectively. As the main focus of this work lies on the development of the track following controller, rear wheel steering is assumed for assuring enough damping of the yaw motion. To be able to judge the capability of robust decoupling the simulations based on a Daimler Benz City Bus 0 305 and a 1986 Pontiac

6000 STE Sedan are compared in sections 5 and 6 with the results presented in (Ackermann and Sienel, 1990) and (Guldner, *et al.*, 1999). For the development of the mentioned controller structure a model for the car is needed first. In this paper the linearized single track model in combination with the bar bell model for the mass distribution is used. Combining these equations with the decoupling controller is content of the next section.

## 2. STEERING DYNAMICS AND ROBUST UNILATERAL DECOUPLING

The basic idea of robust decoupling is to make the lateral acceleration of the car independent of its yaw rate for one single location which is called decoupling point  $DP$ . In this context the term “robust” implies that varying parameters like the velocity of the car ( $v \in [v^-; v^+]$ ), its mass ( $m \in [m^-; m^+]$ ) or the friction coefficient ( $\mu \in [\mu^-; 1]$ )

---

<sup>1</sup> Tel.: ++49-8153-28-2423  
E-mail: juergen.ackermann@dlr.de

do not have any effect on this attribute.

As maneuvers with high lateral acceleration are avoided in the field of automatic car steering the assumption of small sideslip and steering angles and slowly varying velocity is realistic. Under these assumptions the single track model which describes the steering dynamics of the vehicle is

$$\begin{bmatrix} mv(\dot{\beta} + r) \\ J\dot{r} \end{bmatrix} = \begin{bmatrix} 1 & 1 \\ l_F & -l_R \end{bmatrix} \begin{bmatrix} F_{yF} \\ F_{yR} \end{bmatrix} + \begin{bmatrix} F_{yD} \\ M_{zD} \end{bmatrix} \quad (1)$$

where  $\beta$  is the sideslip angle at the center of gravity (CG) and  $r$  describes the yaw rate. The parameter  $l_F$  (respectively  $l_R$ ) is the distance between CG and the front (respectively rear) axle so that  $l = l_F + l_R$  stands for the wheelbase. The velocity  $v$ , the mass  $m$  and the moment of inertia  $J$  of the car are uncertain parameters. The lateral forces  $F_{yF}(\alpha_F)$  and  $F_{yR}(\alpha_R)$  at front and rear axle (sum of left and right wheel forces) are the main uncertainties. They are functions of the front and the rear wheel tire sideslip angles  $\alpha_F$  and  $\alpha_R$ , see figure 2. Transforming the disturbance force  $F_{yD}$  at CG and the disturbance torque  $M_{zD}$  around the  $z$ -axis through CG into  $F_{yDF}$  and  $F_{yDR}$  (disturbance forces at front and rear axle) with

$$\begin{bmatrix} F_{yD} \\ M_{zD} \end{bmatrix} = \begin{bmatrix} 1 & 1 \\ l_F & -l_R \end{bmatrix} \begin{bmatrix} F_{yDF} \\ F_{yDR} \end{bmatrix} \quad (2)$$

the single track model becomes

$$\begin{bmatrix} mv(\dot{\beta} + r) \\ J\dot{r} \end{bmatrix} = \begin{bmatrix} 1 & 1 \\ l_F & -l_R \end{bmatrix} \begin{bmatrix} F_F \\ F_R \end{bmatrix} \quad (3)$$

with

$$\begin{aligned} F_F &:= F_{yF}(\alpha_F) + F_{yDF} \\ F_R &:= F_{yR}(\alpha_R) + F_{yDR} \end{aligned} \quad (4)$$

The so called bar bell model which describes the mass  $m$  and the moment of inertia  $J$  of the car by two rigidly connected point masses  $m_R$  and  $m_{DP}$  is based on the relation

$$\begin{bmatrix} 1 & 1 \\ l_R & -l_{DP} \\ l_R^2 & l_{DP}^2 \end{bmatrix} \begin{bmatrix} m_R \\ m_{DP} \end{bmatrix} = \begin{bmatrix} m \\ 0 \\ J \end{bmatrix} \quad (5)$$

By fixing  $m_R$  at the rear axle (see figure 1), the solution of (5) is made unique and the distance of DP to CG becomes  $l_{DP} = J/ml_R$ .

As shown in (Ackermann, *et al.*, 2002) the lateral acceleration  $a_{yDP}$  at the decoupling point is independent of the side forces at the rear axle. This follows from

$$\begin{aligned} a_{yDP} &= a_{yCG} + l_{DP}\dot{r} \\ &= \frac{(F_F + F_R)}{m} + \frac{l_{DP}(F_F l_F - F_R l_R)}{J} \end{aligned} \quad (6)$$

with

$$\begin{aligned} J &= ml_R l_{DP} \\ a_{yDP} &= \frac{l}{ml_R} F_F \end{aligned} \quad (7)$$

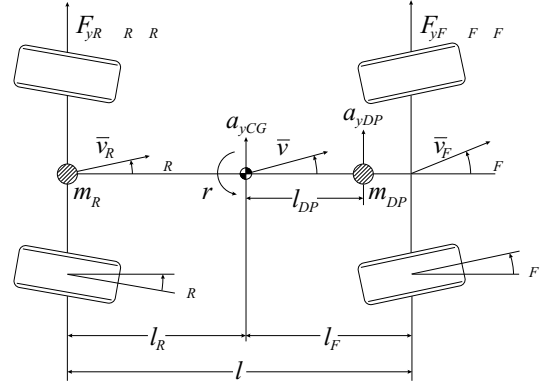


Fig. 1. Parameters of the single track model, definition of the decoupling point

The aim is to make  $\alpha_F$  and thus  $F_F$  and  $a_{yDP}$  independent of the yaw rate  $r$ . It is reached by the following control law (see Ackermann, *et al.*, 2002, and figure 2):

$$\begin{aligned} \delta_F &= \delta_S + \delta_C \\ \dot{\delta}_C &= -r - \frac{l_{DP} - l_F}{v} \dot{r} \end{aligned} \quad (8)$$

$\delta_S$  is the input for the lane following feedback.

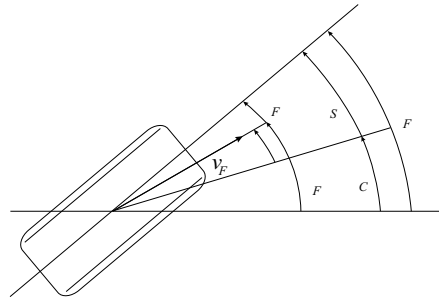


Fig. 2. Angles at the front wheel

For the design process it is helpful to transform the sideslip angle  $\beta$  and the steering angle  $\delta_C$ , which is formed by the decoupling controller, into the sideslip angle  $\beta_R$  at the rear axle and the angle  $\gamma$  by the following equations

$$\begin{aligned} \beta_R &= \beta - \frac{l_R}{v} r \\ \gamma &= \beta_F - \delta_C = \beta + \frac{l_F}{v} r - \delta_C \end{aligned} \quad (9)$$

In the following it is assumed that the tire side forces with their saturation characteristic can be linearized as follows:

$$F_{yF}(\alpha_F) = \mu_C \alpha_F, \quad F_{yR}(\alpha_R) = \mu_C \alpha_R \quad (10)$$

The cornering stiffness  $c_F$  (respectively  $c_R$ ) at front (respectively rear) axle is known. The friction coefficient  $\mu$  is uncertain and varies between  $\mu^-$  (slippery road) and  $\mu^+ = 1$  (dry road). To be able to perform this linearization it must be assured that  $\alpha_F$  and  $\alpha_R$  remain small because in this case the operating point stays in the linear part of the characteristic curve. Using  $\alpha_F = \delta_S - \gamma$  (see figure 2) and  $\alpha_R = \delta_R - \beta_R$  in combination with (3), (7), (8), (9) and (10) the resulting system becomes

$$\begin{bmatrix} \dot{\beta}_R \\ \dot{r} \\ \dot{\gamma} \end{bmatrix} = \begin{bmatrix} a_{11} & -1 & a_{13} \\ a_{21} & 0 & a_{23} \\ 0 & 0 & a_{33} \end{bmatrix} \begin{bmatrix} \beta_R \\ r \\ \gamma \end{bmatrix} + \begin{bmatrix} b_{11} & b_{12} \\ b_{21} & b_{22} \\ b_{31} & 0 \end{bmatrix} \begin{bmatrix} \mu c_F \delta_S + F_{yDF} \\ \mu c_R \delta_R + F_{yDR} \end{bmatrix} \quad (11)$$

with

$$\begin{aligned} a_{11} &= -\frac{\mu c_R (l_{DP} + l_R)}{m v l_{DP}}; & b_{11} &= \frac{l_{DP} - l_F}{m v l_{DP}} \\ a_{13} &= -\frac{\mu c_F (l_{DP} - l_F)}{m v l_{DP}}; & b_{12} &= \frac{l_{DP} + l_R}{m v l_{DP}} \\ a_{21} &= \frac{\mu c_R}{m l_{DP}}; & b_{21} &= \frac{l_F}{m l_R l_{DP}} \\ a_{23} &= -\frac{\mu c_F l_F}{m l_R l_{DP}}; & b_{22} &= -\frac{1}{m l_{DP}} \\ a_{33} &= -\frac{\mu c_F l}{m v l_R}; & b_{31} &= \frac{l}{m v l_R} \end{aligned} \quad (12)$$

The last row in (11) shows that  $\dot{\gamma} = a_{yDP}/v$  is independent of  $\beta_R$ ,  $r$ ,  $\delta_R$  (steering angle at the rear axle) and  $F_{yDR}$ . It is only influenced by  $\delta_S$  (part of the front wheel steering angle  $\delta_F = \delta_C + \delta_S$ , which is generated by the track following controller) and  $F_{yDF}$ . This attribute is emphasized by the characteristic polynomial of (11) which factorizes into two separate parts –  $p_{dec}(s) = p_{lat}(s) \cdot p_{yaw}(s)$  – with

$$\begin{aligned} p_{lat}(s) &= s + \frac{\tilde{\mu} c_F l}{v l_R} \\ p_{yaw}(s) &= s^2 + \frac{\tilde{\mu} c_R (l_{DP} + l_R)}{v l_{DP}} s + \frac{\tilde{\mu} c_R}{l_{DP}} \end{aligned} \quad (13)$$

For the design process there are two uncertain parameters which have to be considered: the velocity  $v \in [v^-; v^+]$  and the friction coefficient normalized by the mass  $m \in [m^-; m^+]$ :

$$\tilde{\mu} = \frac{\mu}{m}, \quad \tilde{\mu} \in \left[ \frac{\mu^-}{m^+}; \frac{1}{m^-} \right] \quad (14)$$

It must be pointed out that an exact robust decoupling controller can have good yaw damping only by the use of rear wheel steering. The main focus of this work lies on the track following controller. Therefore good yaw damping is provided

by the most convenient approach of rear wheel steering. If no rear wheel steering is available, then further compromises must be made (Ackermann *et al.*, 1996). However, in order to achieve realistic simulation results,  $r$  has to be well damped. To solve this task the yaw rate  $r$  (that is measured for the control law (8) anyway) is fed back to the steering angle  $\delta_R$ . The development of this controller which follows (Ackermann, 2003) is content of the next section.

### 3. DAMPING OF THE YAW MOTION

As shown in section 2 the dynamics of the yaw motion is described by  $p_{yaw}(s)$ . Written as the second order standard polynomial

$$p_{yaw}(s) = s^2 + 2D_{dec}\omega_{0dec}s + \omega_{0dec}^2 \quad (15)$$

natural frequency and damping result in

$$\omega_{0dec} = \sqrt{\frac{\tilde{\mu} c_R}{l_{DP}}}; \quad D_{dec} = \frac{l_{DP} + l_R}{2v} \sqrt{\frac{\tilde{\mu} c_R}{l_{DP}}} \quad (16)$$

According to (Ackermann, *et al.*, 2002)  $D_{dec}(\tilde{\mu}, v)$  is smaller than the damping of the uncontrolled car for velocities  $v > v_e$  where  $v_e$  is in the operating domain. In order to enhance  $D_{dec}$  especially for higher velocities, a proportional controller with gain scheduling is proposed (see Ackermann, 2003)

$$\delta_R = -K_R(v)r \quad (17)$$

yielding the characteristic polynomial

$$p_R(s) = s^2 + \frac{\tilde{\mu} c_R}{l_{DP}} \left( \frac{l_{DP} + l_R}{v} - K_R \right) s + \frac{\tilde{\mu} c_R}{l_{DP}} \quad (18)$$

with unchanged natural frequency.

By  $K_R = K_R(v)$  a desired velocity damping

$$D_{des}(\tilde{\mu}^-, v) = \frac{1}{2} \sqrt{\frac{\tilde{\mu}^- c_R}{l_{DP}}} \left[ \frac{l_{DP} + l_R}{v} - K_R(v) \right] \quad (19)$$

can be assigned by

$$K_R(v) = \frac{l_{DP} + l_R}{v} - 2D_{des}(\tilde{\mu}^-, v) \sqrt{\frac{l_{DP}}{\tilde{\mu}^- c_R}} \quad (20)$$

For  $D_{des}$  a linear characteristic is chosen with  $D_{des}(v^-) = D_{dec}(v^-)$  and  $D_{des}(v^+) = 1$ .

After the discussion of the controller stabilizing the yaw rate (which is necessary for the simulations in sections 5 and 6) the main result for the lane tracking controller design is presented in the next section.

#### 4. ROBUST TRACK FOLLOWING CONTROLLER FOR THE CITY BUS

First model (11) is augmented by  $\Delta\psi$  (angle between the track tangent and the vehicle longitudinal orientation) and  $y_{DP}$  (lateral displacement at the decoupling point), see (Ackermann, 2003).

$$\begin{aligned}\Delta\dot{\psi} &= r - v\rho_{ref} \\ \dot{y}_{DP} &= v(\beta_R + \Delta\psi) + (l_R + l_{DP})r\end{aligned}\quad (21)$$

With  $\beta_R$  and  $r$  from (11) the transfer functions for the output  $y_{DP}$  are

$$\begin{aligned}y_{DP}(s) &= \frac{a\tilde{\mu}}{s^2\left(s + \frac{a\tilde{\mu}}{v}\right)}u(s) + \\ &\frac{l/ml_R}{s\left(s + \frac{a\tilde{\mu}}{v}\right)}F_{yDF}(s) - \frac{v^2}{s^2}\rho_{ref}(s)\end{aligned}\quad (22)$$

The second integrator of the first term is caused by a hydraulic cylinder without position feedback for the front wheel steering of the bus so that only  $u = \delta_S$  can be influenced by the controller. For simplification the constant parameter  $a = c_F l / l_R$  is introduced. In the specifications of (Ackermann and Siemel, 1990) it is required that the steady state value of  $y_{DP}$  is zero after a step input in  $F_{yDF}$  which is already guaranteed by the integral behaviour of the cylinder. In order to stabilize the two poles at  $s = 0$  two controller zeros are necessary. Together with two realization poles the controller structure is

$$G_R(s) = \frac{K_0 + K_1 s + K_2 s^2}{s^2/\omega_{0,S}^2 + 2D_S/\omega_{0,S} s + 1}\quad (23)$$

where  $D_S = 0.6$  and  $\omega_{0,S} = 40$  [1/s] are fixed (see Ackermann and Siemel, 1990). The determination of the design parameters  $K_0$ ,  $K_1$  and  $K_2$  was executed with the MATLAB toolbox PARADISE<sup>2</sup>. The theoretical background of this program is the parameter space approach (see Ackermann, *et al.*, 2002): all eigenvalues of the closed loop must be located in a chosen region of the left half of the s-plane which is surrounded by the so called  $\Gamma$ -boundary. In this case the  $\Gamma$ -boundary is a hyperbola with minimal damping  $D_{min} = 0.25$  and maximal real part  $\sigma_{max} = -0.55$ :

$$\left(\frac{\sigma}{0.55}\right)^2 - \left(\frac{\omega}{2.13}\right)^2 = 1\quad (24)$$

The left branch of this hyperbola is mapped now into one of the three possible controller planes via the characteristic polynomial for the four vertices

of the operating domain while the third controller parameter has to be fixed:

$$\begin{aligned}\operatorname{Re} p(\sigma + j\omega, \tilde{\mu}, v) &= 0 \\ \operatorname{Im} p(\sigma + j\omega, \tilde{\mu}, v) &= 0\end{aligned}\quad (25)$$

The intersection of the stable regions leads to a set of parameters which stabilizes the four chosen points and which is a candidate to achieve  $\Gamma$ -stability for the whole operating domain. This has to be checked by mapping the hyperbola into the  $(v, \tilde{\mu})$ -plane. For  $K_0 = 4$ ,  $K_1 = 2$  and  $K_2 = 0.3$  figure 3 shows that the closed loop is  $\Gamma$ -stable according to (24) because no line intersects the interesting area, and the four vertices of the rectangle are  $\Gamma$ -stable by construction.

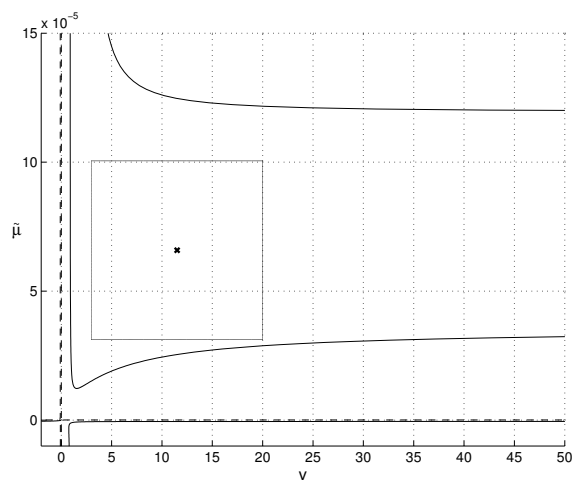


Fig. 3. Stability check of the operating domain

After the development and the parametrization of the controller structure the principle of robust decoupling will be compared to the results of (Ackermann and Siemel, 1990) in the next section.

#### 5. SIMULATION RESULTS FOR THE CITY BUS O 305

The vehicle model, which is used in the simulations, has the parameters:  $c_F = 198000$  N/rad,  $c_R = 470000$  N/rad,  $l_F = 3.67$  m,  $l_R = 1.93$  m,  $\mu \in [0.5; 1]$ ,  $v \in [3; 20]$  m/s,  $m_{min} = 9950$  kg,  $m_{max} = 16000$  kg,  $J(m_{min}) = 105700$  kgm<sup>2</sup>,  $J(m_{max}) = 171300$  kgm<sup>2</sup>. In order to keep things simple, only the two most critical of the four maneuvers described in (Ackermann and Siemel, 1990) are discussed in this paper: driving into a narrow bus stop bay at  $v^- = 3$  m/s and transition from straight line into a circle with curvature  $\rho_{ref} = 0.0025$  m<sup>-1</sup> at  $v^+ = 20$  m/s.

The constraints for these maneuvers are:

$$\begin{aligned}\omega_n &\leq 7.5 \text{ rad/s}; & |\delta_F| &\leq 40 \\ |a_y| &\leq 4 \text{ m/s}^2; & |\dot{\delta}_F| &\leq 23 \text{ s}^{-1} \\ |y| &\leq 15 \text{ cm}\end{aligned}$$

<sup>2</sup> <http://www.robotic.dlr.de/control/paradise>

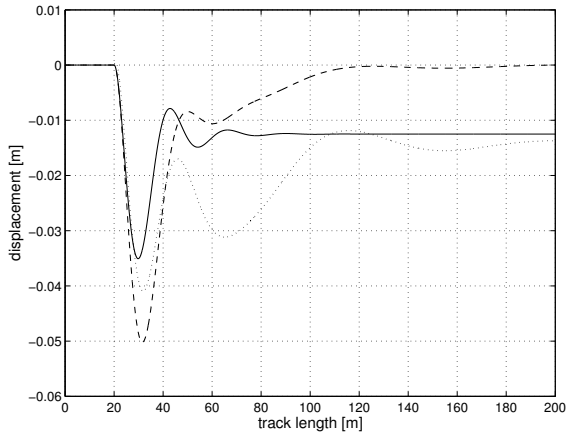


Fig. 4. Transition into the curve ( $\tilde{\mu} = \tilde{\mu}^-$ )

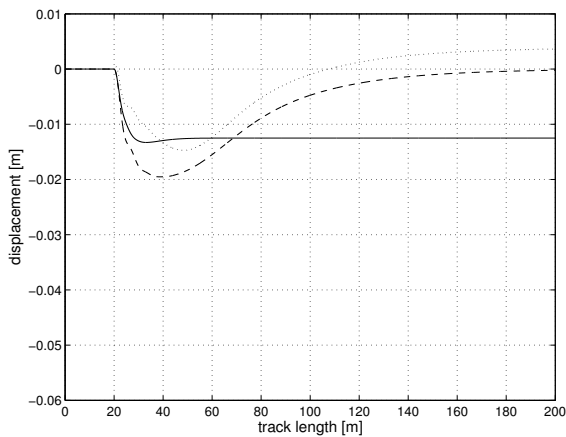


Fig. 5. Transition into the curve ( $\tilde{\mu} = \tilde{\mu}^+$ )

Compared to the displacement at the front sensor of the benchmark bus (dashed line) which is located at  $l_S = 6.12m$  in front of CG, the maximum of  $y_{DP}$  (solid line) at  $l_{DP} \approx 5.50 m$  is smaller for  $\tilde{\mu}^-$  as well as for  $\tilde{\mu}^+$  (see figures 4 and 5). This conclusion is also true for the displacement at  $DP$  of the benchmark bus (dotted line). The relatively low damping of the yaw rate in the results of (Ackermann and Sieneel, 1990) in the case of minimal road adhesion, which is the reason for the sinusoidal characteristic of the dotted line (see figure 4), is improved by the use of rear wheel steering. These improvements can also be noticed in the results for the bus stop bay which cannot be displayed in this paper due to limited space. However, it is not possible for this maneuver to fulfill the constraint regarding the maximal value of  $\delta_F$ . As tests with an ideal feedforward control in this project have revealed that the original requirements can only be met for  $v$  smaller than  $3 m/s$ , this fact is no reason against the idea of robust decoupling. Further simulations have shown that nonlinear tire side force characteristics of saturation type (see Pacejka and Bakker, 1991) have no effect on the stability of the developed controller structure. Therefore the linearization in (10) is valid.

In the next section the idea of robust decoupling is applied to a fast passenger car in order to extend the operating domain towards higher velocities.

## 6. EXTENSION OF THE OPERATING DOMAIN TO HIGHER VELOCITIES

The controller design for the 1986 Pontiac 6000 STE Sedan can be executed in the same way as for the bus. The actuator for front wheel steering is a servo motor now with a real pole at  $10 Hz$  and a complex pole pair at  $5 Hz$  with  $0.4$  damping (see Guldner, *et al.*, 1999). Furthermore it is assumed that its stationary gain is one.

The values of the parameters which are necessary for the simulations are:  $c_F = c_R = 80000 N/rad$ ,  $l_F = 1.10 m$ ,  $l_R = 1.58 m$ ,  $\mu \in [0.5; 1]$ ,  $v \in [4; 40] m/s$ ,  $m = 1573 kg$ ,  $J = 2873 kgm^2$ .

Due to the fact that the same requirements with respect to steady state tracking error after step inputs in  $F_{yDF}$  and  $\rho_{ref}$  are stated as in the last section, the controller has to include the integrator which has been the cylinder in the case of the city bus. With a second realization pole the structure for the track following controller is:

$$G_{R,P}(s) = \frac{K_{0,P} + K_{1,P}s + K_{2,P}s^2}{s(s/\omega_{0,P} + 1)} \quad (26)$$

with  $\omega_{0,P} = 4\pi$  (see Guldner, *et al.*, 1999).

To guarantee  $D_{min} = 0.4$  and  $\sigma_{max} = -0.5$  of the specified hyperbola in the whole operating domain, gain scheduling is necessary in which the velocity  $v$  of the car is the parameter. In the design process with PARADISE tolerance bands have been determined for  $K_{0,P}$ ,  $K_{1,P}$  and  $K_{2,P}$ . With regard to minimization of steady state tracking error for curve riding the upper boundaries of the mentioned bands have to be the goal for the gain scheduling (see e.g. figure 6). Due to the form of these boundaries hyperbolic functions are convenient to describe the  $v$ -characteristic of the controller parameters particularly for high velocities. As the boundaries for  $K_{2,P}$  are determined in view of reasonable stability regions in the  $(K_{0,P}, K_{1,P})$ -plane the tolerance band can slightly be exceeded without losing  $\Gamma$ -stability. For the simulations in this section the following functions are chosen:

$$\begin{aligned} K_{0,P}(K_{1,P}) &= 2 \cdot K_{1,P} - 0.16 \\ K_{1,P}(v) &= 5.60/v + 0.13 \\ K_{2,P}(v) &= 0.40/v + 0.08 \end{aligned} \quad (27)$$

The linear dependency between  $K_{1,P}$  and  $K_{0,P}$  is helpful to keep the design process more simple.

Approximating the track of the benchmark paper which consists of a straight section followed by a right turn, a left turn, another right turn and a final straight section, the test maneuver is given.

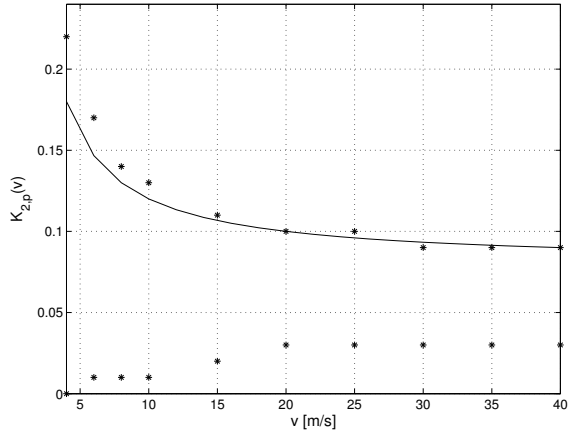


Fig. 6. Gain scheduling for  $K_{2,P}(v)$

The radius of the curves is  $R_{ref} = 800 \text{ m}$  with  $\rho_{ref} > 0$  for left curves and the transition points are  $t_1 = 18 \text{ s}$ ,  $t_2 = 25 \text{ s}$ ,  $t_3 = 39 \text{ s}$  and  $t_4 = 46 \text{ s}$  for  $v = 35 \text{ m/s}$ . The developed controller structure is compared to the ideal state control law of (Guldner, *et al.*, 1999) in figures 7 and 8 which show the lateral displacement at the decoupling point (solid line), the lateral displacement at the front sensor (dashed line) and at the decoupling point (dotted line) of the benchmark results. For  $\tilde{\mu}^-$  the maximal values and the steady state errors are further reduced. As the displacement signal for  $\tilde{\mu}^+$  is very similar to the results of the ideal state controller in (Guldner, *et al.*, 1999) (which is not realizable in this form because the derivatives of the displacement signals at front and rear bumper are needed) it can be noticed that the idea of robust decoupling is also useful for fast passenger cars.

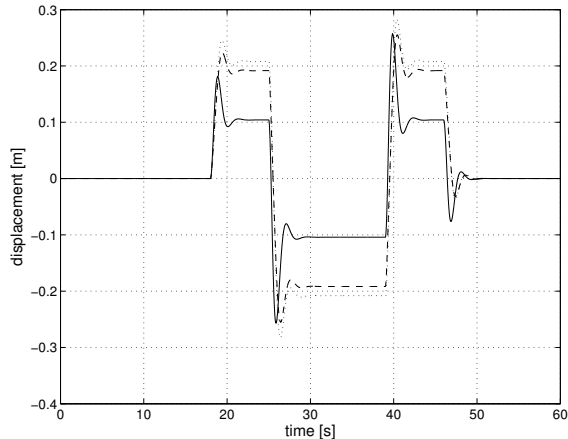


Fig. 7. Test track ( $\tilde{\mu} = \tilde{\mu}^-$ )

## 7. SUMMARY

Comparing robust decoupling control with different approaches for automatic car steering it can be seen that the design process is easier due to splitting into the two subtasks “lane tracking” and

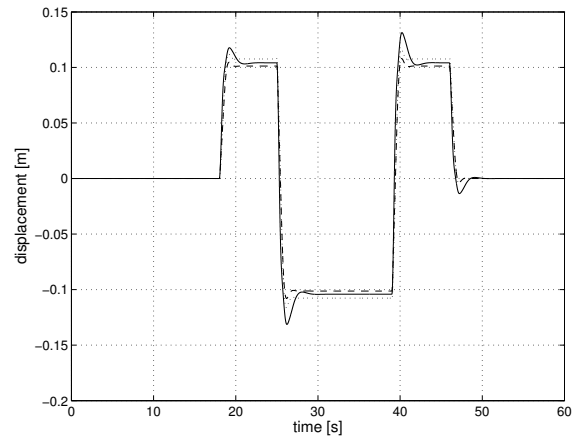


Fig. 8. Test track ( $\tilde{\mu} = \tilde{\mu}^+$ )

“damping of the yaw rate” which are independent if rear wheel steering is assumed. For the city bus the maximal values of the lateral displacement can be reduced and the degree of controller numerator and denominator can be decreased by one. Applying the idea to fast passenger cars it can be seen that the accuracy of the track following controller is enhanced especially for minimal road adhesion.

## REFERENCES

- Ackermann J. (2003). *A Three-step-design Procedure for Automatic Car Steering*. DLR Interner Bericht Nr. 515-03-03, Oberpfaffenhofen.
- Ackermann J., Blue P., Bunte T., Güvenc L., Kaesbauer D., Kordt M., Muhler M., Odenthal D. (2002). *Robust Control: The Parameter Space Approach*. Springer, London.
- Ackermann J., Bunte T., Sienel W., Jeebe H., Naab K. (1996). *Safety by robust steering control*. Proc. Int. Symposium on Advanced Vehicle Control (Aachen), **vol. 1**, pp. 377-394.
- Ackermann J., Sienel W. (1990). *Robust Control for Automatic Steering*. Proc. American Control Conference (San Diego), pp. 795-800.
- Guldner J., Sienel W., Tan H.-S., Ackermann J., Patwardhan S., Bunte T. (1999). *Robust automatic steering control for look-down reference systems with front and rear sensors*. IEEE Trans. on Control Systems Technology, **vol. 7**, no. 1, pp. 2-11.
- Pacejka H.B., Bakker E. (1991). *The magic formula tyre model*. Proc. 1st Int. Colloquium on Tyre Models for Vehicle Dynamic Analysis, Swets & Zeitlinger, Amsterdam/Lisse, pp. 1-18.